Two-fluid analysis of the thermal-hydraulic stability of ITER CS and TF super-conductors

R.Zanino, C.Marinucci (*) and L.Savoldi

Dipartimento di Energetica, Politecnico, I-10129 Torino, Italy
(*) CRPP Fusion Technology Division, CH-5232 Villigen PSI, Switzerland

Thermal-hydraulic stability of the two-channel cable-in-conduit conductors (CICC) foreseen for the central solenoid (CS) and the toroidal field (TF) Nb3Sn super-conducting coils of the International Thermonuclear Experimental Reactor (ITER) is analyzed with the two-fluid code MITHRANDIR [1]. In all external-heating scenarios considered, the computed stability margin is of the order of some 100 mJ/ccst. Extra-strands Cu addition typically leads to higher computed margins. MITHRANDIR estimates are typically conservative with respect to one-fluid results.

1 INTRODUCTION

The International Thermonuclear Experimental Reactor (ITER) is being designed to be the first tokamak to reach ignition and sustained burn. Plasma confinement is achieved by means of super-conducting magnets, consisting of several subsystems: the central solenoid (CS), the toroidal field (TF) coils, and the poloidal field (PF) coils. These magnets can be subject to different types of thermal loads (nuclear, mechanical, electromagnetic, etc.) and an assessment of their thermal-hydraulic stability is essential for the operation of the machine.

One peculiarity of the cable-in-conduit conductors (CICC) designed for ITER is that they have a two-channel topology. The cables are wound in an annular region (bundle) around a central channel (hole), which provides pressure exhaust in case of a quench and lower hydraulic impedance for the supercritical helium coolant. A new code - MITHRANDIR - was recently [1] developed for the analysis of thermal-hydraulic transients in two-channel CICC. MITHRANDIR implements a one-dimensional (*x* co-ordinate along the conductor) two-fluid model allowing for different flow *and thermodynamic state* of the helium in the bundle and hole regions. On the contrary, in standard one-fluid models, e.g., GANDALF, the same pressures and temperatures are assumed in the two regions. All strands are assumed to carry the same current density, and the external disturbance is applied uniformly in the conductor cross-section, i.e., electromagnetic effects [2] are not included, for the present, in either code.

MITHRANDIR was applied to a first study of heat slug propagation in the QUench Experiment on Long Length (QUELL) in [3], and very recently it was validated against QUELL quench data [4], showing in both cases good agreement, typically better than GANDALF, with the experiment. QUELL stability was also analyzed [5] indicating significant differences between the predictions of the two codes. Here we present some results of a detailed two-fluid stability analysis of the ITER CS and TF conductors using the MITHRANDIR code.

2 DEFINITION OF DISTURBANCE SCENARIOS

Each of the scenarios considered here (see Table 1) corresponds to a different duration τ_Q and length IHZ of the external heating pulse Q_0 [W/m], which is deposited directly into the conductor at its center. All details on the definition of conductor parameters can be found in [6].

Two different cases, TF1 and TF2, have been considered for the TF conductor, whereas three, CS1, CS2 and CS3, have been considered for the CS conductor. Some of these scenarios qualitatively correspond to specific physical origins of the disturbance: the TF1 case corresponds to a mechanical disturbance (micro slips of individual strands [7]), whereas the TF2 and CS3 correspond to AC losses subsequent to a plasma disruption. The other scenarios are used for code benchmarking purposes.

	TF1	TF2	CS1	CS2	CS3
IHZ [m]	1	15	12	12	150
τ_Q [ms]	1	100	1	100	100

Table 1 Disturbance scenarios

3 ESTIMATES OF STABILITY THRESHOLDS

The computed stability thresholds are reported in Table 2 in terms of mJ/ccst. Values in parentheses were obtained with the 1-fluid GANDALF code [8-9]. The arithmetic average (below briefly referred to as average threshold) between maximum energy for recovery and minimum energy for quench is given. The implementation of the quench/recovery stability criterion in MITHRANDIR is discussed in [6]. In the case of extra Cu, the values in Table 2 have been computed from the input parameter Q_0 using only the cross-section area of Cu in strands.

	TF1	TF2	CS1	CS2
Cu in strands only	333 (565)	230 (238)	293 (310)	260 (253)
Cu in strands + extra	863 (1314)	241 (238)	355 (463)	364 (406)

Table 2 Average stability thresholds [mJ/ccst] obtained with the 2-fluid MITHRANDIR code. Values in parentheses from the 1-fluid GANDALF code [8-9]. The thresholds for the CS3 scenario are not reported here because spatial oscillations appear in the solution with both code [6,8].

A detailed (and very CPU demanding) convergence study (presented in [6]) was performed for Cu in strands only and its results were then used for extra Cu. For each scenario separately, the numerical parameters were determined (i.e., element size Δx in the uniform refined mesh around the external heater, and constant time step Δt) leading to reliable estimates of the margin. A *numerical dual stability threshold* is found, e.g., in the CS1 case with Δt=5.e-6s, using Δx=36mm, while finer $\Delta x \leq 18$mm is needed to obtain the result of Table 2. The spatial oscillations in the CS3 scenario are being subject to further investigation.

The margins computed with MITHRANDIR are rather conservative with respect to estimated losses in the conductors. In the TF1 case, e.g., a 10 mJ/ccst loss is estimated [7], whereas in the TF2/CS3 case the loss is estimated in the worst case around 80-120 mJ/ccst [7].

The comparison with the 1-fluid results from GANDALF shows that the 2-fluid estimates are typically conservative as expected. The bundle-hole coupling time scale can be estimated as $\tau_{BH} \sim (T/|T_B - T_H|)$ $(\rho C_p A/h_{BH} P) \sim 1$ (1e2 1e3 1e-4/h_{BH} 1e-2) ~ (1e3/ h_{BH}) ~ 0.1-1 s. The difference in the predicted margins is small or negligible in the scenarios (TF2, CS1, CS2) with $t_{END} \leq \tau_{BH}$ (see below and [6]), while it becomes significant in the TF1 scenario ($t_{END} << \tau_{BH}$). The smaller differences found here between the two models with respect to the QUELL case [5] can also be partly explained by the smaller relative value of the hole cross-section area in this case (~10% for TF, ~20% for CS vs. ~30% for QUELL).

3.1 Qualitative analysis of the different scenarios

The effects of different disturbances on the stability of the conductor can be distinguished considering the time evolution of the normal zone (NZ) length as in Figs.1a-d, for both the minimum Q_0 for quench and the maximum Q_0 for recovery.

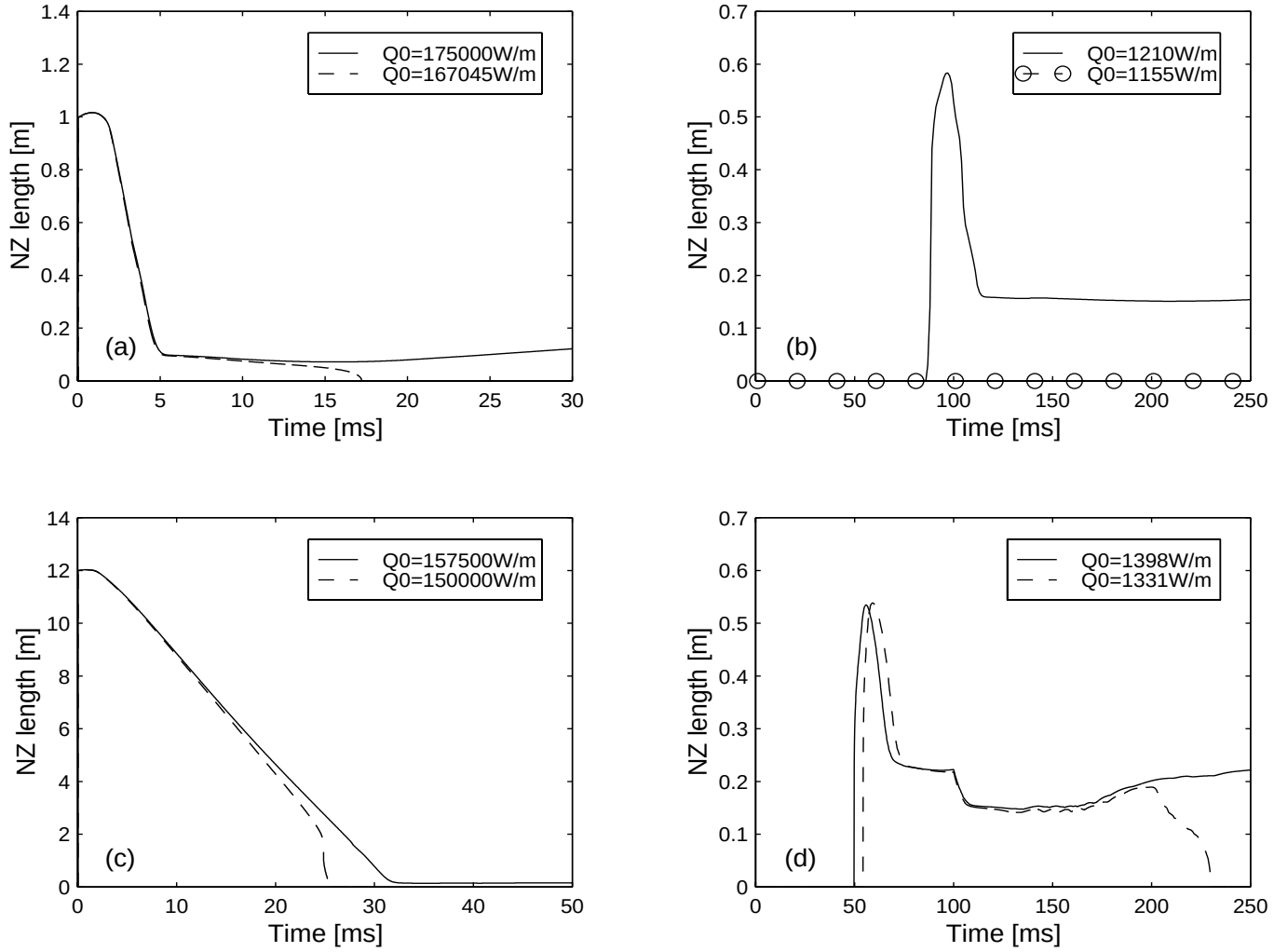

Figure 1 Converged time evolution of normal zone length initiated by maximum external linear power input Q_0 for recovery (solid lines) and minimum Q_0 for quench (dashed lines). Scenarios: TF1 (a), TF2 (b), CS1 (c), CS2 (d).

In all scenarios the power input Q_0 into the conductor causes a sudden increase of bundle helium pressure p_B and hole helium pressure p_H in the IHZ, through the heat transfer coefficient *H* between conductor and bundle helium [1]. Steep fronts build up near the edge of the IHZ in the early stage of the transient and induce ($\rho\, \partial V/\partial t \propto -\partial p/\partial x$) a strong flow reversal near the left edge and a strong flow near the right edge, with $|V_{induced}| > |V_{operation}|$. In the meanwhile the perturbation fronts start moving (and broadening) upstream and downstream respectively. The induced bundle and hole helium speeds V_B and V_H, are almost equal during this phase, notwithstanding the big difference in the hydraulic impedance of the two regions. Friction effects appear indeed only on the longer time scale $\tau_f \sim D/(fV)$, where D is the hydraulic diameter and *f* is the friction factor. The induced flow in the bundle modifies in turn the steady state heat transfer coefficient h_{Nu} between bundle helium and conductor, which feeds back on *H* [1].

Besides τ_Q two additional time scales appear to influence the different details of the NZ evolution in the different scenarios, based on the previously discussed mechanism:

1. the time $\tau_Z \sim IHZ/C_S$ needed by the perturbation to reach the center of the IHZ;
2. the time τ_{Nu} needed for the transient contribution to *H*, $h_t \propto 1/\sqrt{t}$, to decay below h_{Nu}, i.e., for the flow perturbation to feed back onto the conductor temperature T_{co}.

In both the TF1 (Fig.1a) and the CS1 (Fig.1c) scenario NZ ~ IHZ almost instantaneously. This is related to the fact that for both scenarios $\tau_{Nu} >> \tau_Q$ (for the CS1 additionally $\tau_Z >> \tau_Q$). Therefore, the heat transfer coefficient increase due to the induced flow does not improve the cooling of the conductor fast enough, while it is being externally heated. During the following evolution the NZ shrinks progressively while the perturbation fronts move towards the center of the IHZ. Therefore the quench/recovery "decision" can be actually taken only at $t = t_{END} \geq \tau_Z$.

In both the TF2 (Fig.1b) and the CS2 (Fig.1d) scenarios, on the other hand, $\tau_Z \sim \tau_Q$ and $\tau_{Nu} < \tau_Q$. This qualitatively explains why, for Q_0 near the threshold, the quench starts over a short region (<< IHZ) near the center of the IHZ, i.e., when the two perturbation fronts are about to meet. The rest of the IHZ is, by that time, well cooled by the induced flow.

4 EFFECTS OF EXTRA-STRANDS COPPER

The simulations indicate that extra Cu in the conductor provides increased stability (see Table 1). Indeed, the Cu cross section area in the conductor, A_{Cu}, enters *directly* three entirely different terms in the model equations [1]: a) Joule power generation P_J in the conductor; b) Heat capacity of the conductor; c) Heat conductivity of the conductor. Among these one finds by careful analysis [6] that as A_{Cu} is sufficiently increased the dominant role is played by the decrease of P_J, which obviously leads to increased threshold.

The computed gain is very different depending on the scenario (compare TF1 and TF2). Also, the increase in threshold is much larger in the CS2 than in the TF2 scenario, although the relative increase in Cu is significantly larger for the TF conductor than for the CS [6]. In both cases the differences are due to the *fortuitous* very small increase in threshold for the TF2 scenario. The TF2 would not behave much differently than the TF1 if only more Cu was added in the conductor [6].

5 CONCLUSIONS AND PERSPECTIVE

The computed stability margins for all external heating scenarios considered here are all well above 200mJ/ccst, i.e., the ITER TF and CS design appears to be conservative from this point of view. Extra Cu typically leads to a higher margin. Two-fluid MITHRANDIR estimates turn out to be conservative in most cases as expected, when compared with one-fluid GANDALF results.

In perspective we believe that the model must be validated against *measurements* of the stability margin, which are however essentially unavailable at present for two-channel CICC. The model should also be improved, e.g., by including electromagnetic effects and implementing improved transient heat transfer coefficients.

Some major issues have not been addressed in this paper, e.g., numerical convergence study, peculiarity of the CS3 scenario, and effects of bundle-hole coupling parameters in the two fluid model. All of these points were preliminarily discussed in [6] and shall be presented elsewhere.

6 ACKNOWLEDGEMENTS

The European Community through contracts NET/96-424 (to R.Z.) and NET/96-425 (to C.M.) partially financially supported this work.

7 REFERENCES

[1] Zanino, R., DePalo, S. and Bottura, L. J.Fus.Energy (1995) 14 25
[2] M.Shimada and N.Mitchell, J.Fus.Energy (1995) 14 59
[3] Zanino, R., Bottura, L. and Marinucci, C. IEEE Trans. Appl. Supercond. (1997) 7 493
[4] Zanino, R., Bottura, L. and Marinucci, C. Adv. Cryo. Eng. (1998) 43 181
[5] DePalo, S., Marinucci, C. and Zanino, R. Adv. Cryo. Eng. (1998) 43 333
[6] Zanino, R. and Savoldi, L. Politecnico di Torino Report PT DE 478/IN (April 1998)
[7] P.Bruzzone, to appear in IEEE Trans. Mag. (1998)
[8] Marinucci, C. EPFL Report CRPP/FT/CM/98-RE-01 (May 1998)
[9] Marinucci, C., Savoldi, L. and Zanino, R. to be presented at ASC98